Journal of Applied Polymer Science

Manufacturing and characterization of polyether ether ketone/methyl phenyl polysiloxane composite coatings

Massimiliano Barletta,[1] A. Gisario,[2] M. Puopolo,[1,3] S. Vesco[1]

[1]Dipartimento di Ingegneria dell'Impresa, Università degli Studi di Roma "Tor Vergata", via del Politecnico, 1, Roma 00133, Italy
[2]Dipartimento di Ingegneria Meccanica e Aerospaziale, "Sapienza" Università di Roma, via Eudossiana, 18, Roma 00184, Italy
[3]Polymer Technology Center, Mechanical Engineering Department, College station, Texas A&M University, Texas 77843-3123
Correspondence to: M. Barletta (E-mail: barletta@ing.uniroma2.it)

ABSTRACT: In this work, manufacturing and characterization of single- and multilayer polyether ether ketone (PEEK)-reinforced coatings were investigated. Hybrid composites of thermoplastic reinforcing agents in a thermoset resin was, therefore, achieved by dispersing large PEEK particles (~85 μm diameter) in methyl phenyl polysiloxane (MPP). First, mechanism of formation of the polymeric networks during MPP curing at different temperatures (250–400 °C) was analyzed. The different arrangements of the PEEK powders inside the cross-linked network of the MPP resin were, thus, disclosed. Second, the effect of process parameters on visual appearance, morphological features, and mechanical response of the composite coatings was evaluated by contact gauge profilometry, scanning electron microscopy, IR spectrometry, and microscratch indentations. Moderate temperature curing (250 °C > T > 300 °C) of the composite coatings led to polysiloxane resins harder, well adhered on the metal and able to retain better the PEEK reinforce. Further increase in curing temperature (350 and 400 °C) might embrittle the polysiloxane resin, with the PEEK powders in it partially attenuating the loss of properties of the composite coating. © 2016 Wiley Periodicals, Inc. J. Appl. Polym. Sci. **2016**, *133*, 43609.

KEYWORDS: coatings; compatibilization; cross-linking; manufacturing

Received 9 January 2016; accepted 6 March 2016
DOI: 10.1002/app.43609

INTRODUCTION

Polyether ether ketone (PEEK) is an excellent but expensive polymeric material, which is particularly useful to protect metallic surfaces in erosive–corrosive environments, especially in the presence of relatively high temperature.[1] PEEK might be deposited on metal substrates by a number of different technologies as thermal spraying,[2–5] printing,[6] or electrophoretic deposition.[7,8] These routes always imply time-consuming procedures, are often extremely expensive, and require specific equipments. In addition, the resulting PEEK coatings might feature limited performance because of the poor adhesion of the thermoplastic material on the metal substrate. Thermal spraying is generally acknowledged as the most viable solution to deposit PEEK powders on metals. It involves the propulsion of partially softened PEEK powders toward the target (usually, a metal substrate). The powders are softened by combustion or plasma and, at the same time, directed to the target by a high-pressure air or gas jet.[3] The partially softened PEEK particles deform (i.e., flatten) after impinging the target surface and, rapidly, cool off and consolidate in the forms of oblong splats.[9] Therefore, the progressive superimposition of the splats on the target generates the growth of the coating. Nevertheless, thermal spraying often forms highly defective coatings, characterized by low homogeneity and occasional porosities. Crystallization of the polymer can also be a serious issue, as it depends on cooling of the material during the substrate impact, which is very troublesome to control. Crystallization degree of the polymer can severely influence the final properties of the coatings, especially their adhesion to the substrate and wear resistance.[3,6,10] Annealing or thermal post-treatment of the thermally sprayed coatings and appropriate preparation of the substrate surface are thus often necessary to restore the material properties[11] or promote the coating–substrate interfacial adhesion.[12–14] Obviously, the additional treatments have high costs, which are often unacceptable, being PEEK powders extremely expensive. Substrate pretreatments by steel grit blasting, degreasing, and chemical etching prior to thermal spraying of PEEK powders on AISI 304 stainless steel were investigated by Patel *et al.*[14] They found the corrugation of the metal might increase the adhesion with the PEEK coatings by the mechanical interlocking of the asperities on the metal surface with the polymer. Laser post-treatments of the coatings might result in the compaction of the PEEK layers after thermal spraying.[3] However, laser processing of the coatings requires multiple laser scans and accurate calibration of the irradiation

parameters to prevent preferential energy absorption on coating imperfections that might cause the local degradation of the material. In addition, laser processing is intrinsically not homogeneous because of the difference in power density between the center and edges of the laser spot, which can significantly affect the effectiveness of the treatment on the coating surface.

PEEK powders could be applied on metal after dispersion in a liquid medium, for example, a thermosetting resin. This would lead to the formation of a composite material that might be deposited on the target by conventional spraying. Consolidation of the coating might be achieved by the high-temperature curing of the resin after the deposition process. While the preparation of PEEK-based composite cannot be considered a novelty in itself, the idea of driving PEEK powders on metal by the dispersion in a liquid and thermally curable resin has never been explored before. However, other attempts to combine thermoplastic and thermosetting resins abound in the literature. In 1995, Frigione *et al.* blended a polystyrene filler inside an epoxy resin.[15] Apparent incompatibility of the two phases drove the formation of an interphase constituted by part of the thermosetting monomers being embedded in the bulk of the thermoplastic phase. Similarly, by heating up the composite material, part of the thermoplastic material was found to diffuse in the thermosetting resin. The resulting composite was found to feature intermediate properties between the thermosetting and thermoplastic fraction. Pham *et al.* found that toughness of epoxy resin was improved using a thermoplastic filler of high affinity with the thermosetting resin like butadiene and its copolymers with acrylonitrile.[16] More recently, Ollier *et al.* reported that the presence of a thermoplastic, such as polycaprolactone, inside a thermosetting vinyl ester, can improve toughness, stiffness, and fracture properties of the composite.[17] Composites based on polysiloxane resin have also been recently investigated in the recent literature. Jiang *et al.* reported a composite in which polyester-grafted sericite was dispersed in dimethyl silicone resin.[18] Lee *et al.* reported on the role of poly(methylsilsesquioxane)s as silicone matrix.[19]

These encouraging results about blending of compatible and incompatible thermoplastic and thermosetting fractions as well as the need for a facile route to deposit PEEK powders on metal has therefore inspired this work. PEEK powders are herein dispersed inside a thermosetting matrix, that is, a hybrid organic–inorganic methyl phenyl polysiloxane resin (MPP). MPP resins boast a high affinity with most of metals by the formation of covalent bonds per hydrolysis and condensation reactions.[20–22] Therefore, MPP resins should ensure a stronger adhesion of the PEEK–MPP composite with the metal substrate. Moreover, the high chemical affinity of MPP and PEEK, due to the presence of phenyl groups on the lateral chains of the polysiloxane backbone, should ensure a strong interaction between the two materials, even without the onset of covalent bonds. The achievement of a PEEK–MPP composite would thus allow designing a new material, whose properties are a compromise between affinity to metal, high chemical inertness, and hardness of MPP with excellent thermal, wear, and abrasion resistance of PEEK. In this respect, manufacturing of single- and multilayer PEEK-reinforced MPP coatings was investigated. Large PEEK particles (~80 μm diameter) were dispersed in the thermosetting resin. The effect of process and curing parameters on visual appearance, morphological features, and mechanical response of the coatings was evaluated. Experimental findings show that curing of MPP might promote the establishment of a composite material very hard and tough, well adhered on the metal and able to retain effectively the PEEK reinforcing phase. The composite materials were found to ensure extremely interesting thermal and mechanical properties, especially when tested in severe operating conditions.

EXPERIMENTAL

Materials

Fe 430 B steel substrates, 40 mm long, 30 mm wide and 5 mm thick, were coated by the PEEK/MPP composite material. Therefore, the matrix of the composite material is an MPP thermosetting resin (Evonik, Essen, Germany) functionalized with hydroxyl and alkoxy groups lateral groups. In the starting formulation, propane-1,2,3 triol (approximately 10 wt %) is added to the MPP resin to favor the cross-linking process by the condensation reaction of the glycerol function groups with the hydroxyl counterparts on the siloxane chains. The reinforcing filler, that is, the PEEK particles, ~85 μm average diameter of the granulometric distribution, was provided by Victrex (Lancashire, United Kingdom). Almost 100% of the granulometric distribution is over 10 μm.

Manufacturing Process

The steel substrates were ground by a lapping machine (Abramin, Struers, Milan) to obtain a fairly smooth and homogenous starting surface morphology. Grinding process was performed for 2 min on each substrate using P80 abrasive paper (240 μm abrasive granule size) at 150 rpm. Pretreated metal substrates were immediately washed with water and acetone and, once dried, they were dipped 1 min in an alkaline solution at temperature of 70 °C. After that, the substrates were rinsed with bidistilled water and dried to prevent oxidation.

Table I summarizes the experimental schedule. Pretreated substrates were sprayed with an air-mix gun (feeding pressure 2.5 bar, nozzle 1 mm, stand-off distance 400 mm, spray gun inclination ~45°) with the MPP resin alone and, subsequently, with the PEEK (15 wt %)/MPP composite material. Dispersion of the PEEK in MPP was promoted by diluting the resin in acetone with a 1:2 dilution ratio. After dilution, PEEK powders were added and mixed thoroughly to ensure good dispersion. Spraying was calibrated to achieve thickness of 50 ± 10 and 110 ± 10 μm, respectively. Coatings thickness and their uniformity were measured by a Palmer micrometre (Mitutoyo, 0–25 mm measuring range, ± 2 μm sensitivity, 0.001 mm resolution) performing three measurements equally distributed over the coated surface. All the samples whose thickness felt out of the prescribed range were not considered further.

After coating, the samples were predried for 30 min at 60 °C and subsequently baked in a preheated (250–400 °C) convection oven (Nabertherm P330, Lilienthal, Germany) for 45 min to cross-link the polysiloxane resin. A set of samples was recoated

Table I. Experimental Schedule

Coating codes	Types	Thickness (μm)	T (°C)
R250	MPP	50 ± 10	250
R300	MPP	50 ± 10	300
R350	MPP	50 ± 10	350
R400	MPP	50 ± 10	400
P250	MPP + PEEK	110 ± 10	250
P300	MPP + PEEK	110 ± 10	300
P350	MPP + PEEK	110 ± 10	350
P400	MPP + PEEK	110 ± 10	400
T250	MPP + PEEK + MPP	110 ± 10	250
T300	MPP + PEEK + MPP	110 ± 10	300
T350	MPP + PEEK + MPP	110 ± 10	350
T400	MPP + PEEK + MPP	110 ± 10	400

with an additional layer of MPP for sealing purposes. In this case, the application of the second layer of MPP was followed by a predrying at 60 °C for 30 min and an additional curing step for 45 min in the preheated (250–400 °C) convection oven. Being the PEEK melting point of ~340 °C, curing temperatures were chosen to cover a wide range around the peak melting point of PEEK.

Experimental Procedures

Differential scanning calorimetry (Netzsch, DSC200PC, Selb, Germany) was performed on PEEK samples, heating the polymer from ambient temperature up to 450 °C, with a scanning rate of 5 °C/min. FTIR analysis (FT-IR 4000 Jasco) was performed to evaluate the curing mechanisms, the presence of eventual interactions between thermosetting resin and thermoplastic filler and assess the potential degradation of the PEEK or MPP resin after curing process. Heat degradation resistance was evaluated recording IR spectra on PEEK or MPP after curing for 45 min at different temperatures: 250, 300, 350, and 400 °C. FTIR spectra was acquired in ATR mode in a spectral range of 4000–600 cm^{-1} with a resolution of 2 cm^{-1} and a sampling rate of 64 scans min^{-1}.

Coatings morphology was measured by contact inductive gauge of a CLI profiler (TalySurf CLI 2000, Taylor Hobson, Leicester, UK). An area 4 × 4 mm^2 was covered storing for each sample 2000 profiles, 4 mm long at a resolution of 2 µm along the measurement direction. TalyMap 3.1 software allowed elaborating stored profiles and the main roughness parameters R_a and R_z evaluation. Visual appearance and morphology of the coatings were examined by a field Emission Gun–Scanning Electron Microscope (FEG-SEM Leo, Supra 35, Carl Zeiss SMT, Inc. Thornwood, New York). Coating adhesion to the substrate was evaluated by the Cross Cut test according to the ASTM D3359 regulation.

Progressive load scratch tests (Micro-Combi, CSM Instruments, Peseaux, Switzerland) were performed using a rounded conical Rockwell C-type diamond indenter, with 800-µm-tip radius, 1 mm/min sliding speed, 100 mN to 30 N incremental load, 3 mm scratch pattern. During the test, the indenter first profiled the surface with a very low load applied recording the starting surface profile (i.e., prescan). Then, the tip, sliding at constant speed, penetrated the coating material applying the load required to the achievement of the scratch pattern (i.e., scan). Normal and tangential forces were recorded. Finally, the indenter profiled back the scratch pattern at low load recording the changes in coating morphology leftover after the material elastic recovery. At this stage, the residual depth (i.e., postscan) was stored. This allowed the rebuilding of the residual scratch pattern by the contact inductive gauge of the surface profiler to evaluate the size and geometry of the residual scratch patterns. Scanning electron microscopy allowed examining the morphology of the residual scratch patterns.

EXPERIMENTAL RESULTS

Manufacturing of the Coatings and Characterization of the Chemical Structures

DSC of PEEK powders is reported in Figure 1. The material shows a small recrystallization peak at ~155 °C and a peak melting point at ~340 °C. A small inflection of the DSC trend at ~145 °C is associated to the glass transition temperature of the PEEK in agreement with Ref. 23. The peak melting point of the PEEK found at ~340 °C has suggested the setting of the curing temperatures of the coatings. They were chosen in the range of 250–400 °C. Two values were taken below the peak melting point (250 and 300 °C) and two above it (350 and 400 °C). All the curing temperatures were high enough to activate the network formation of the MPP resin according to what suggested by the resin manufacturers. In the former case (i.e., temperatures below the peak melting point), the resulting coatings are, therefore, conventional composites in which the unmolten PEEK reinforcing agent is dispersed in the cross-linked MPP resin. Adhesion between the two fractions is only ensured by the good chemical affinity between polymer particles and MPP thermosetting resin. In the latter case (i.e., temperatures above the peak melting point), the molten or partially molten PEEK powders could mix intimately with the thermosetting resin, especially during the initial stage of the curing

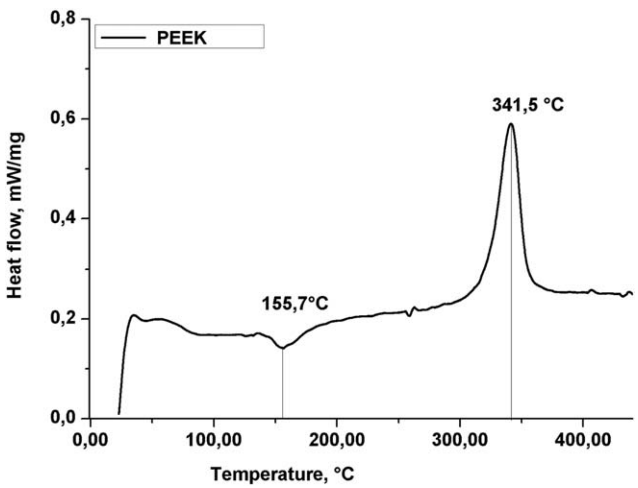

Figure 1. Differential scanning calorimetry of PEEK powders.

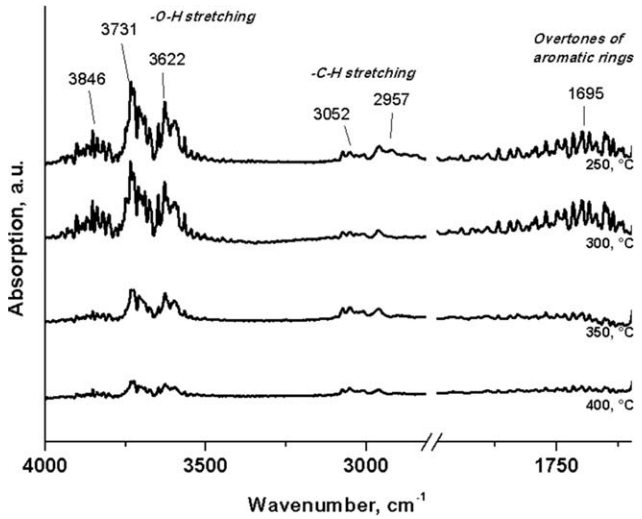

Figure 2. FTIR spectra of the MPP resin cured at different curing temperature (4000–1600 cm^{-1}).

process. This should led to the formation of an "interphase" region between the two materials in agreement with Ref. 24. This interphase, supposed to be constituted by the semimolten thermoplastic polymer embedded in the moieties of thermosetting resin after the formation of the network, should favor the merging of the two materials, thus giving rise to a more homogenous material.

Figures 2–4 report the FTIR analysis of the MPP resin after curing at 250, 300, 350, and 400 °C. Figure 2 refers to the wavenumbers in the range of 4000–1600 cm^{-1}. Stretching absorptions of hydroxyl groups of the MPP resin and of the glycerol can be seen in the range of 4000–3500 cm^{-1} in agreement with Ref. 25. At approximately 3000 cm^{-1}, the weak signal of the stretching bands of C—H bonds in the glycerol and of the methyl and phenyl groups in the MPP resin can be observed. Last, in the range of 2000–1700 cm^{-1}, the overtones of the aromatic groups of the MPP resin can be seen in agreement with Ref. 26. Increasing the temperature, the degree of reaction by the condensation route of the silanol groups (weakening of the signal attributed to the hydroxyl groups in the range of 4000–3500 cm^{-1}) increases significantly. The decrease of the signal in the range of 2000–1700 cm^{-1} at temperatures of 350 and, above all, 400 °C can be ascribed to the thermal degradation of the phenyl groups on the polysiloxane chains. Even the methyl groups underwent a certain thermal degradation as seen by the slight reduction in the signal of C—H bonds at temperature above 350 °C. Figure 3 refers to the range of 1600–900 cm^{-1}. The stretching bands of the Si—O bonds are very strong. They can be found in the range of 1130–1011 cm^{-1}. As expected, the corresponding bands increase with the increase in curing temperature. This change is attributable to the increase in the degree of achievable cross-linking of the MPP resin when cured at higher temperatures through the condensation reactions. In the range of 1500–1400 cm^{-1} and at temperature of 250 and 300 °C, the signals of asymmetric deformation of methyl groups linked to the silicon of the polysiloxane chains are found. They are superimposed to the overtone signals of the aromatic groups linked to silicon.[27] At temperatures of 350 and 400 °C, the signal of asymmetric deformation disappears. Accordingly, at the highest temperatures, the overtone signals of the aromatic groups can be seen again. Disappearance of the signal of asymmetric deformation of the methyl groups is attributed to a change in the configuration of the molecules rather than to thermal degradation of methyl groups in agreement with Refs 26,27. In fact, the peak at 1257 cm^{-1}, typical of the methyl groups linked to silicon, is always enough strong whatever the curing temperature. This result confirms a significant presence of these groups even after curing of the MPP resin at the highest temperatures. However, a slight decrease in the peak at 1257 cm^{-1} at 400 °C supports the hypothesis of a weak degradation of the methyl groups when the highest curing temperature is chosen. Figure 4 refers to the wavenumber of 900–600 cm^{-1}. At ~843 cm^{-1}, the stretching of Si—H bonds and, similarly, the stretching of Si—C bonds (with

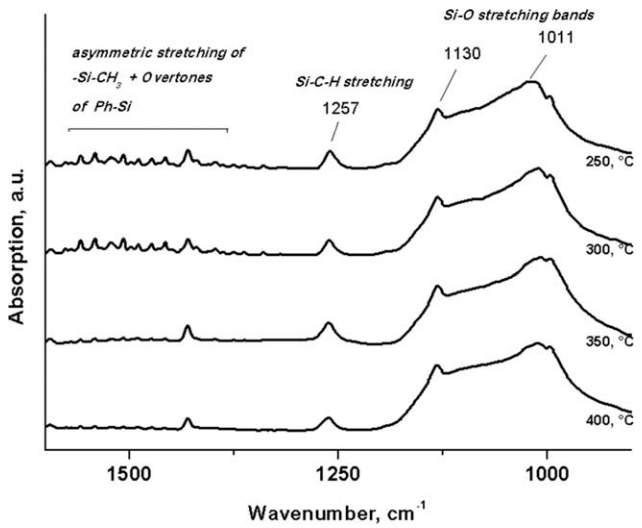

Figure 3. FTIR spectra of the MPP resin cured at different curing temperature (1600–900 cm^{-1}).

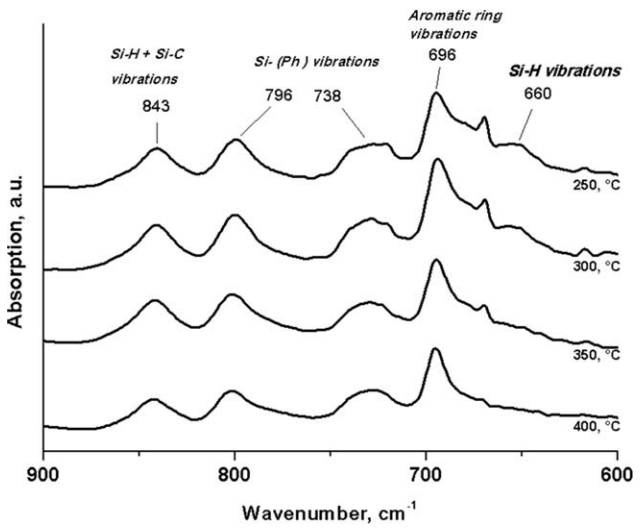

Figure 4. FTIR spectra of the MPP resin cured at different curing temperature (900–600 cm^{-1}).

C belonging to the methyl groups) can be seen. These absorptions should be expected at ~890 cm^{-1}. Nevertheless, the presence of the thermoplastic PEEK powders and the cross-linked structure of the MPP network can probably produce a significant shift of these peaks as found in Ref. 28. The vibrations of aromatic groups linked to silicon can be seen at 796 and 738 cm^{-1} in agreement with Ref. 29. The strong signal at 696 cm^{-1} can be attributed to the vibration of the aromatic rings as shown in Ref. 30. The peaks in the range of 900–600 cm^{-1} are not strictly related to the curing temperature. Nevertheless, close to 660 cm^{-1}, a shoulder peak changes progressively its shape with the curing temperature. In particular, this signal tends to increase by increasing the curing temperature. Accordingly, this signal is ascribable to the formation of additional Si—O—Si bonds at high curing temperature, probably by the oxidation reaction of the Si—H bonds featured on the side of the polysiloxane chains of the MPP resin.

FTIR spectra of MPP resin after curing at progressively increasing temperature show that thermal degradation of the organic fraction of the resin is always moderate. This result is in good agreement with the experimental findings in Ref. 31, where the onset of thermal degradation was found at temperature of 400 °C and higher. Nevertheless, this is in partial contradiction on what claimed by Ref. 32, first, and, above all,[29] later. In these studies, thermal degradation of the MPP resin took place at lower temperature. However, thermal resistance of MPP resin is known to be related to its chemical composition and, in this case, a very good thermal stability is found.

Figure 5 schematizes the reaction of the MPP resins with the glycerol and the additional curing mechanisms. Moreover, it depicts the arrangement of the coating structure according to the curing temperature. Figure 5(a) refers to the curing temperature of 250 °C. The main curing mechanism of the resin is attributable to the condensation reaction of the glycerol with the hydroxyl groups on the chains of the polysiloxane resin. At 250 °C, the temperature is rather low and the PEEK powders do not change their geometry (Figure 6). However, they may remain trapped inside the moieties of the cured MPP resin. Similar mechanisms can be highlighted when curing temperature of 300 °C are set [Figure 5(b)]. The increase in temperature favors an additional reaction mechanism between mutual hydroxyl groups sticking out from different polysiloxane chains, with the formation of an oxygen bridge (i.e., —Si—O—Si— bonds). A partial flattening of the PEEK powders can occur at 300 °C, despite the temperature is still rather lower than the peak melting temperature of the material. Flattening is ascribed to the action of the shrinking resin on the semimolten PEEK powders (they are well above their glass transition point). When the MPP resin cross-links, it assumes new geometrical arrangements and the resin shrinks. Shrinking of the resin causes a rather high contact pressure on the side of the softened PEEK powders, thus inducing a change in its geometrical shape. Figure 5(c) shows the curing mechanisms occurring at 350 °C. Curing takes place by either reaction of the glycerol with the side hydroxyl groups of the polysiloxane chains or by the reaction of the mutual hydroxyl groups featured by the different polysiloxane chains. In addition, PEEK powders start to melt significantly ($T > 340$ °C, peak melting point of PEEK). Under the action of the shrinking resin, the PEEK powders can assume adaptive geometrical configurations, which obviously favor their entrapment in the moieties of the MPP resin during curing process. At 400 °C, an additional reaction mechanism is inferred, that is, the oxidation of lateral hydrogens of the polysiloxane chains and formation of additional oxygen bridges between different polysiloxane chains [Figure 5(d)]. At 400 °C, melting of the PEEK powders is favored (Figure 7), promoting their adaptive entrapment inside the moieties of the MPP resin. Additional space in the cured resin is generated by the thermal degradation of some phenyl and methyl groups and the expected formation of radicals, which can be of certain relevance at 400 °C as seen by FTIR analysis.

Figure 8 reports the FTIR spectra of the PEEK powders after heating at the different temperatures (250–400 °C). PEEK is extremely thermally stable and chemically inert, with some modification only occurring at the highest curing temperature of 400 °C. In agreement with Refs. 33–35, the FTIR analysis allowed to identify the characteristic functional groups of the thermoplastic material. Aromatic C—H absorption bands are visible in the range from 3100 to 2900 cm^{-1}, stretching vibrational mode of the boundary carbonyl groups is observed at 1651 cm^{-1}, skeletal vibration bands in the finger print region at 1593, 1485, 1410 cm^{-1}, and the in-plane deformation of the aromatic C—H appearing as a triplets with bands at 1215, 1183, and 1150 cm^{-1} are detectable. Diphenyl ketone adsorption band is well visible at 925 cm^{-1}. Heating of the PEEK samples at 250, 300, and 350 °C do not imply significant shift of the peaks. On the contrary, heating at 400 °C do imply significant changes in the FTIR spectra. Occurrence of absorption bands at 1740 cm^{-1} and 1366 cm^{-1} can be noticed [Figure 8(b)]. The first band is ascribable to the formation of new carbonyl groups, evidence of polymer degradation. New groups originate from the rupture of the bonds between carbonyl and in α carbons as shown in Ref. 9, followed by their reaction as radicals with the atmospheric oxygen in agreement with Ref. 35. Occurrence of the band at 1366 cm^{-1} can be attributed to polymer degradation, being evidence of the onset of ester-like structures. Decrease in crystalline fraction of the polymer is associated to its degradation, as well. Decrease in crystalline fraction is deduced by the coalescence of a double peak in the fingerprint region at 1305/1276 and 1109/1097 cm^{-1}. The comparison between FTIR spectra of the MPP and PEEK + MPP coatings does not reveal any interaction between them in the range of the curing temperatures investigated (Figure 9). The spectrum of PEEK + MPP composite coatings is given by the composition of the individual spectra of the MPP resin and PEEK powders.

Visual Appearance of the Composite Coatings

Figure 10 shows the visual appearance of the coatings at lower magnification (100×). Continuous coatings can be generally achieved, setting the curing temperature in the range of 250–400 °C. The samples R400 and T400, whose outermost layer is composed of the MPP resin alone, show significant fractures on the coating surface. Temperature of 400 °C is, thus, a superior threshold for the curing process. At 400 °C and after 45 min curing time, the MPP resin features a high degree of cross-

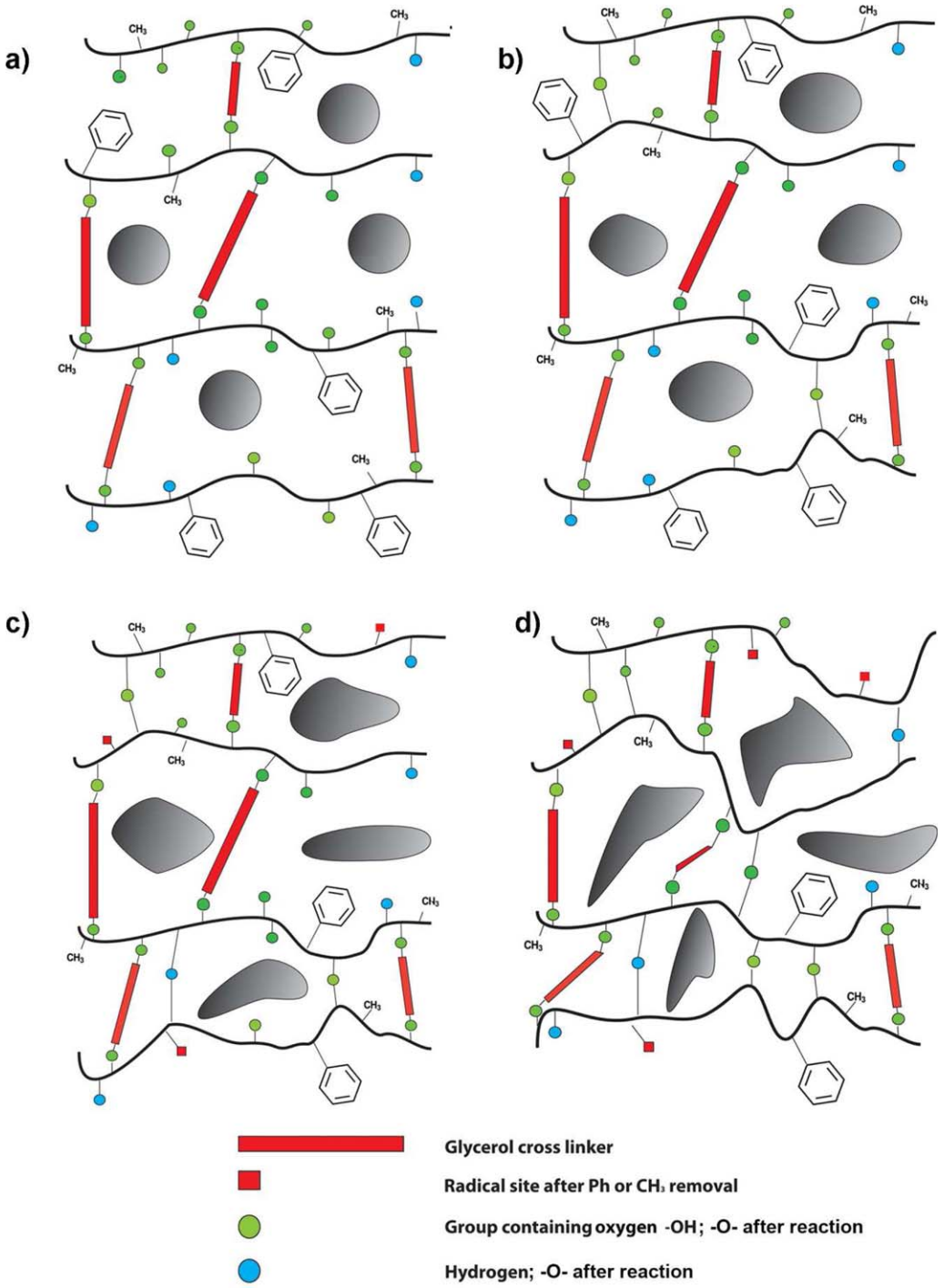

Figure 5. Geometrical arrangements of the composite coatings varying the curing temperature: (a) 250 °C; (b) 300 °C; (c) 350 °C; (d) 400 °C. [Color figure can be viewed in the online issue, which is available at wileyonlinelibrary.com.]

linking in agreement with Refs. 16,17,24. This leads to a material characterized by a high brittleness as reported in Ref. 36,37. In addition, high-temperature curing for long time leads to the mineralization of the polysiloxane resin as emphasized in the FTIR spectra commented in the previous section. High-curing temperature might cause the degradation of the organic fractions (especially, methyl and phenyl groups) on the lateral chains of the polysiloxanes backbone. This leaves on the polysiloxanes backbone some reactive vacancies (especially, radicals), which can, in turn, combine again and form Si—O—Si bonds, thus increasing the glassy behavior of the material, as Keijman *et al.* also found on MPP resin.[38] Accordingly, the MPP resin alone (i.e., sample R) or as topcoat on the underlying layer of PEEK–MPP composite (i.e, sample T) exhibits a brittle failure during high-temperature curing (400 °C) and subsequent cooling off because of the glassy microstructure and severe residual

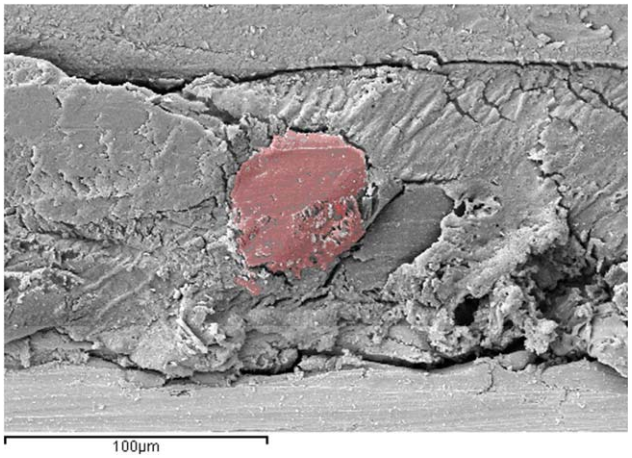

Figure 6. SEM images of a PEEK powder inside a layer of MPP resin after curing at 250 °C. [Color figure can be viewed in the online issue, which is available at wileyonlinelibrary.com.]

stresses arising inside the coating. During thermal curing, MPP resin shrinks much more than metal substrate, thus failing by the formation of large surface cracks (Figure 10, samples R400 and T400) as a result of the prevalently glassy-like microstructure. The presence of the thermoplastic PEEK reinforcing agents in the MPP resin is helpful to oppose the residual stresses in the material, allowing the coating to withstand better the internal stresses arising at that high-curing temperature and retarding or avoiding the onset of large surface cracks as in the sample P400 (Figure 10, sample P400). On the opposite side, temperature of 250 °C is the inferior threshold for curing process as it is imposed by the formation of the MPP network in reasonable processing time.

Figure 11 shows the SEM images of the coatings (i.e., higher magnification) under different curing conditions. High affinity of the polysiloxane resins on the Fe430 B substrates produces uniform and homogenous coatings, well adhered to metal in agreement with Ref. 20, whatever the settings of the curing parameters. This is the case of the samples R (line 1, Figure 11), in which the MPP resin is used alone. The composite coatings PEEK + MPP (samples P) show a corrugated morphology (line 2 Figure 11), in which the PEEK powders protrude from the coating surface in agreement with Ref. 39. PEEK powders are completely surrounded by the MPP resin, which wet the thermoplastic polymer and adhere intimately on it. This result can be attributed to the high affinity between PEEK and MPP, attributable to the common presence of phenyl groups. Curing temperature can influence the morphology of the coatings, especially in the case of PEEK + MPP composites. Curing at 250 and 300 °C is not able to affect the shape of the PEEK powders by melting. Curing at 350 and, especially, at 400 °C could potentially cause the coalescence of the single PEEK powders and their leveling, thus inducing the establishment of flatter coatings morphology. Slow melting kinetic of the PEEK powders as well as the extremely high cross-linking rate of the MPP during curing at 350 and, especially, at 400 °C prevent the PEEK powders to melt completely. Indeed, the thermoplastic powders remain entrapped inside the MPP tridimensional network which is formed rather quickly during curing, thus causing the formation of rather bulky agglomerates. Long-time exposure (45 min curing time) of the composite material at high temperature of 350 and 400 °C is therefore not sufficient to produce a complete leveling (flattening) of the coating morphology by the modification of these PEEK–MPP agglomerates. High-curing temperature of the 400 °C is also expected to promote the formation of an interphase between PEEK powders and MPP resin, especially during the early stage of cross-linking of the MPP in agreement with the experimental findings in Ref. 24. The interphase cannot be detected by FTIR, being merely a phase in which the composite material features different proportion of PEEK and MPP, being them mixed intimately together rather than being dispersed one (i.e., the PEEK powders) in the other (i.e., the MPP resin). These interphases are expected to be particularly prone to withstand high temperature and keep their structure unchanged even after long time exposition at relatively high temperature (350–400 °C).

Samples T in which the MPP resin is used as topcoat on the PEEK–MPP composite (line 3, Figure 11) features a rather smooth morphology. In this case, the MPP topcoat, being driven by the large presence of the diluent in the formulation, is sufficient to infiltrate among the protruding PEEK powders of the underlying layer, level the spaces among them and reduce the surface asperities. Curing temperature is not able to influence significantly the coating morphology.

Figure 12 reports the 3D morphology of the coatings as achieved by 3D contact gauge profilometry. These maps provide information on the *z*-axis, that is, on the height of the morphological features of the coatings. As earlier mentioned, the 3d maps show that an increase in curing temperatures up to 400 °C are not sufficient to produce a significant flattening of the coatings morphology. Figure 13 reports the related roughness parameters. Samples R show average roughness R_a of approximately 0.1 μm with negligible deviations, regardless the curing temperatures. Samples P show average roughness R_a of approximately 14–18 μm. Increase in roughness is

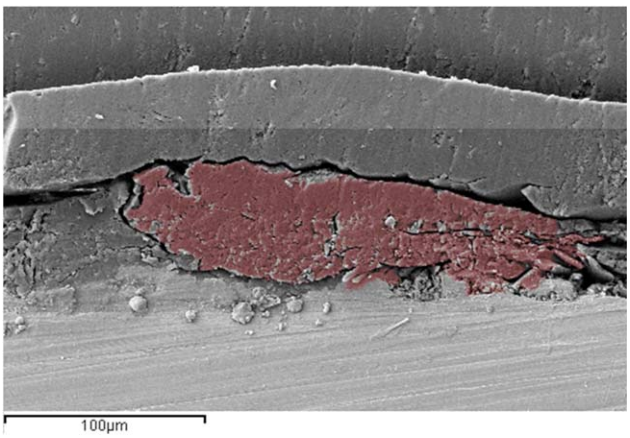

Figure 7. SEM images of a significantly flattened PEEK powder inside a layer of MPP resin after curing at 400 °C. [Color figure can be viewed in the online issue, which is available at wileyonlinelibrary.com.]

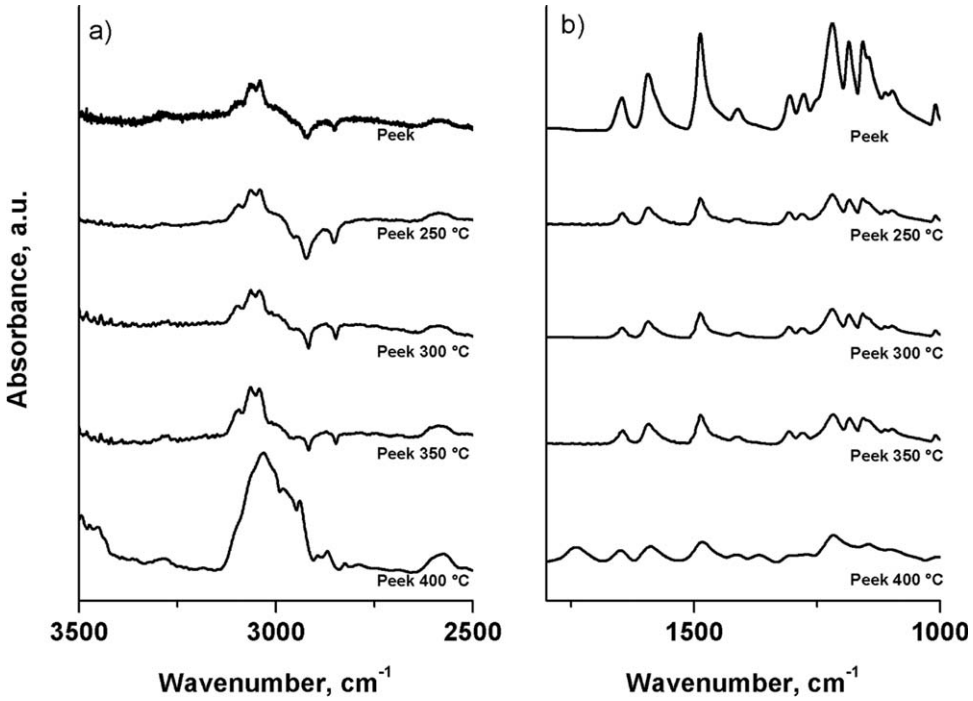

Figure 8. FTIR spectra of PEEK before and after the heating process at 250, 300, 350, and 400 °C: (3a) wavenumbers 3500–2500 cm^{-1}; (3b) wavenumbers 1800–1000 cm^{-1}.

primarily due to the agglomeration of the PEEK particles, which, as said before, protrude from the baseline of the coatings. Samples T show average roughness R_a of approximately 1 μm, with small deviations, which are attributable to the intrinsic variability of the manufacturing process. In this case, the infiltration of the MPP topcoat among the asperities of the PEEK powders protruding from the underlying layer reduces the coarseness of the surface morphology.

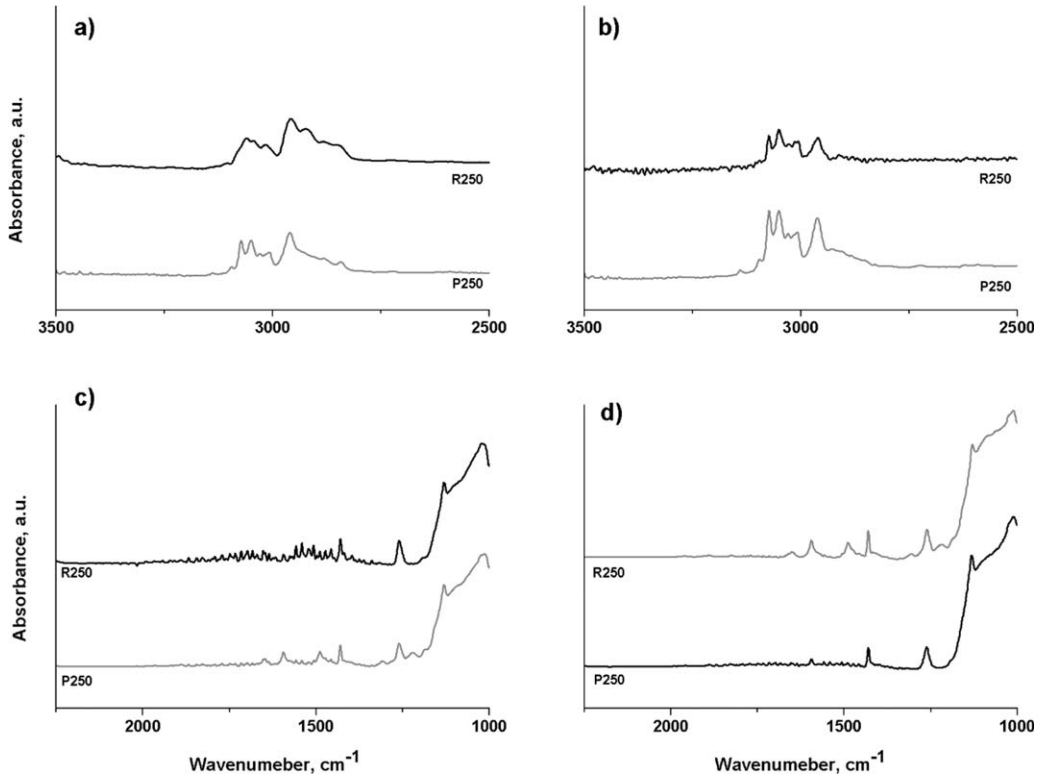

Figure 9. FTIR spectra of the MPP resin and of the PEEK–MPP composite after heating at 250 and 400 °C: (a), (c) R250 and P250C; (b), (d) R400 and P400.

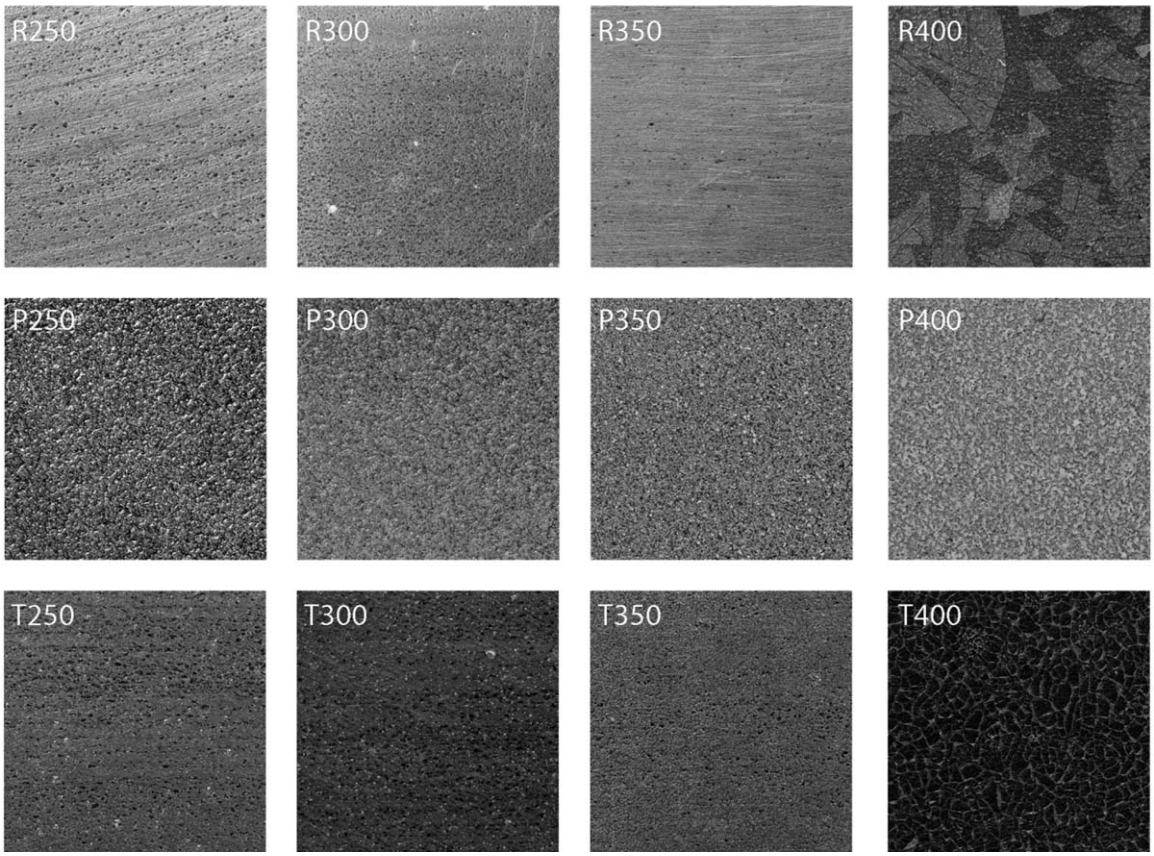

Figure 10. SEM micrographs of the morphology of the coatings.

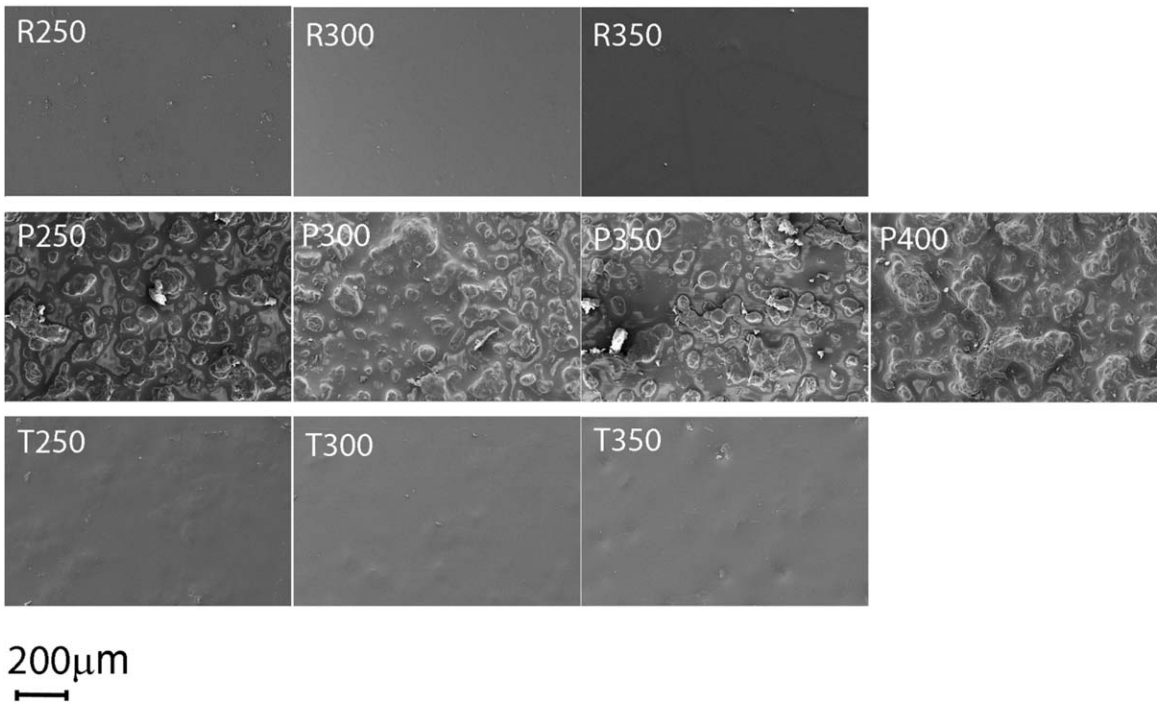

Figure 11. Visual appearance of the samples R400 and T400 after curing process at 400 °C.

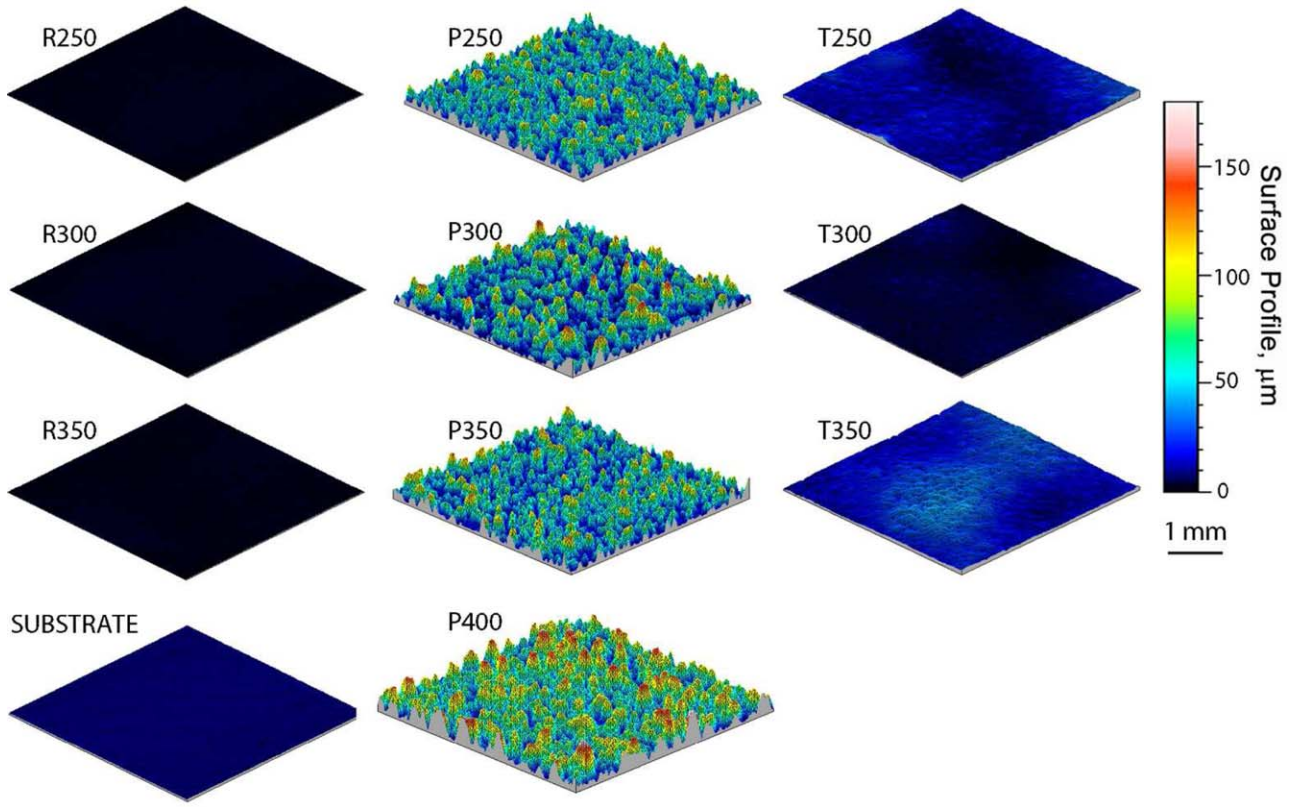

Figure 12. 3D maps of the morphology of the coatings. [Color figure can be viewed in the online issue, which is available at wileyonlinelibrary.com.]

Mechanical Response of the Coatings

Coatings Adhesion. Adhesion of the coatings to the metal substrate was evaluated by cross-cutting tests, according to the ASTM D3359 regulation. Figure 14 shows the coatings after the scratching procedure. All the coatings can be classified as 5B since the test does not produce any delamination. Adhesion is one of the major problems for PEEK coatings on metals, when PEEK is deposited by thermal spraying, printing, or electrodeposition,[4] thus pushing toward the introduction of metal pretreatments or thermal post-treatments of the coatings. Driving the PEEK powders by a diluted liquid resin and applying it on the metals by spraying offer a facile route to overcome adhesion issues between PEEK and most of metals, thus allowing to achieve compact, dense, and well-adhered layers.

Progressive Load Scratch Tests of the MPP Coatings. Figure 15 shows the SEM images of the residual scratch patterns after progressive load scratch tests of the coatings with the indenter tip radius of 800 μm and an increasing load from 0 to 30 N. The residual scratch patterns on the samples R (MPP resin alone) show the typical drop-shaped profile, with an accumulation of plastically deformed material (i.e., pile-up) along the edges of the patterns and in correspondence of the last contact position between indenter and coating material. MPP resin shows a rather ductile response, strongly influenced by the curing temperature. At curing temperature of 250 °C, MPP resin shows the onset of cracking phenomenon already at intermediate loads (~18 N). A set of small C-shaped cracks is formed in the bottom of the scratch pattern, with the hump of the "C"-cracks opposite to the advancing direction of the indenter. This fracture profile corresponds to the failure mechanism by tensile cracking and is typical of an elastic–plastic scratch response of the tested material as reported in Ref. 40. An increase in curing temperature to 300 °C causes a slight hardening of the MPP resin. The residual scratch pattern of the sample R300 still shows a drop-shaped profile, with a minor amount of coating material being plastically displaced around the edges of the track. The critical load (approximately 18 N) is comparable with the one found on sample R250, with fractures being induced by the same mechanism (i.e., tensile cracking). The increase in coating stiffness with less plastic deformation is the result of the higher curing temperature. This means a more complex 3d network of the MPP resin is formed during curing at 300 °C and, accordingly, the material is less prone to deform permanently under the action of the advancing indenter. The sample R350 is even stiffer. It is cross-linked at 350 °C and this produces a very stiff network of the MPP resin. The internal surface of the residual scratch pattern appears undamaged even at the highest normal load (30 N). The accumulation of plastically displaced material around the edges of the residual scratch pattern is almost negligible. Accordingly, the improved scratch resistance exhibited by the sample R350 can be attributed to the increase in curing temperature. Increased curing temperature causes high degree of cross-linking of the MPP resin and, as said before, its significant mineralization by the degradation of part of the organic chains of the siloxanes backbone and recombination of the vacancies with the formation of new covalent Si—O—Si bonds. High-curing temperature can thus induce the

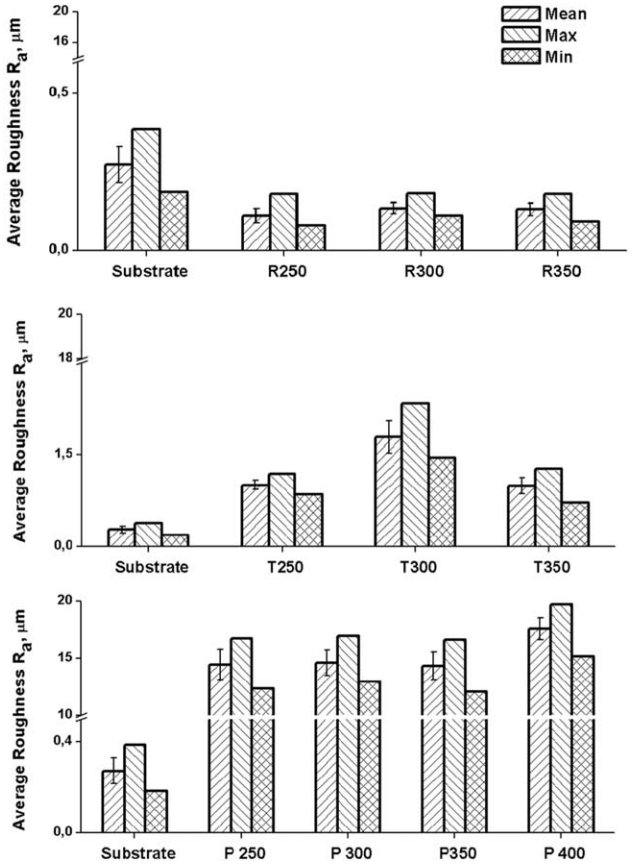

Figure 13. Trends of the roughness amplitude parameters of the as-received substrates and after the deposition on them of the protective coatings.

thermal degradation of the phenyl and methyl groups on the lateral chains of the backbone of the MPP resin, that are responsible of polymer flexibility as found in Ref. 20. The vacant places left on the backbone of the MPP resin are prone to react each other leading to a denser molecular structure and, consequently, forming a stiffer material. A similar effect is induced by the promotion, at high temperature, of the hydrolysis and condensation reactions among hydroxyl groups dislocated along the backbone of the MPP resin and their hydroxyl counterparts on the metal substrates as reported in Ref. 41. Therefore, high-curing temperature might lead to improved interfacial adhesion between coating and underlying metal by the formation of covalent bonds and, thus, to an increased resistance toward external loads as shown in Ref. 20. Curing mechanisms with the formation of 3d complex network inside MPP resin, mineralization reactions inside the resin and combination of the resin with the metal surface confers the MPP coatings a glassy like microstructure, with minimal residual deformation during progressive load scratch tests, high mechanical resistance, and stiffness.

Figure 16(a,b) reports the trends of penetration depths for samples R. The penetration depths show a power-like trend, with the maximum value of penetration of 45 μm being found for the sample R250, that is, the coating cured at the lowest temperature of 250 °C. Maximum penetration depths of ~35 μm were found for the samples R300 and R350, after curing at the higher temperature of 300 and 350 °C. The decrease in the maximum value of penetration depth is obviously connected with the increase in stiffness caused by aforementioned reaction mechanisms.

Progressive Load Scratch Tests of the PEEK–MPP Composite Coatings. SEM images of residual scratch patterns of PEEK–MPP composite coatings are reported in Figure 15 (Line 2). Coatings morphology influences the scratch response of the composite material. At the lowest curing temperature of 250 °C, the presence of PEEK particles, dispersed in the resin, caused a decrease in the coating cohesive strength and reduced its adhesion to the substrate. Accordingly, sample P250 underwent coating delamination, which started at very low applied load. Despite the moderate PEEK content (15 wt %) in the resin,[8] at 250 °C curing temperature, MPP is not able to retain sufficiently the reinforcing agent. This generates discontinuity at the interface, especially of the PEEK powders with the metal substrate. In addition, 250 °C is not enough to promote the onset of the interphase between PEEK and MPP and potentiate their adhesion. For this reason, the PEEK reinforcing agent cannot proficiently contribute to the adhesion and formation of the coating in agreement with the result in Ref. 4. Residual scratch patterns of the sample P300 and P350 are different. They do not show failure onset or delamination from the underlying metal substrate. PEEK powders which protrude from the coating surface are ploughed (i.e., flattened) by the advancing indenter tip. MPP resin in the samples P300 and P350 should feature a high degree of cross-linking because of the higher curing temperature (300 and 350 °C) and increased level of mineralization, which contribute to the improvement of the cohesive strength of the coatings and of their adhesion to metal. Curing temperature of 400 °C leads to further improvement of the scratch response of the composite coating. The sample P400 shows a smaller residual scratch pattern, with the onset of plastic deformation taking place at higher loads. In this case, the improvement of scratch response can be attributed to the further increase in the cross-linking degree after curing at 400 °C and the increase in the extent of the mineralization reactions. Moreover, the highest curing temperature of 400 °C, the thermoplastic reinforcing agent can form aggregates with the MPP resin, forming an interphase, which confer homogeneity and cohesion to the coating in agreement with Ref. 42. It could also be speculated that the presence of an interphase between the potentially ductile thermoplastic fraction with the stiffer MPP resin can lead to an increase in coating toughness and contrast the increased brittleness induced by the mineralization reactions. Figure 16(c,d) reports the trends of the penetration depths for the PEEK–MPP composite coatings. However, the high influence of the coating morphology hidden the actual trends of the penetration depths, not allowing to extract information about scratch response of the coatings.

Progressive Load Scratch Tests of the PEEK–MPP Composite Coatings with the MPP Topcoats. SEM images of residual scratch patterns of the double-layered coatings in which an MPP topcoat is deposited on the innermost PEEK–MPP layer are reported in Figure 15 (Line 3). The residual scratch patterns are very close to those achieved on the MPP coatings. They feature the typical drop-shaped profile, with an accumulation of

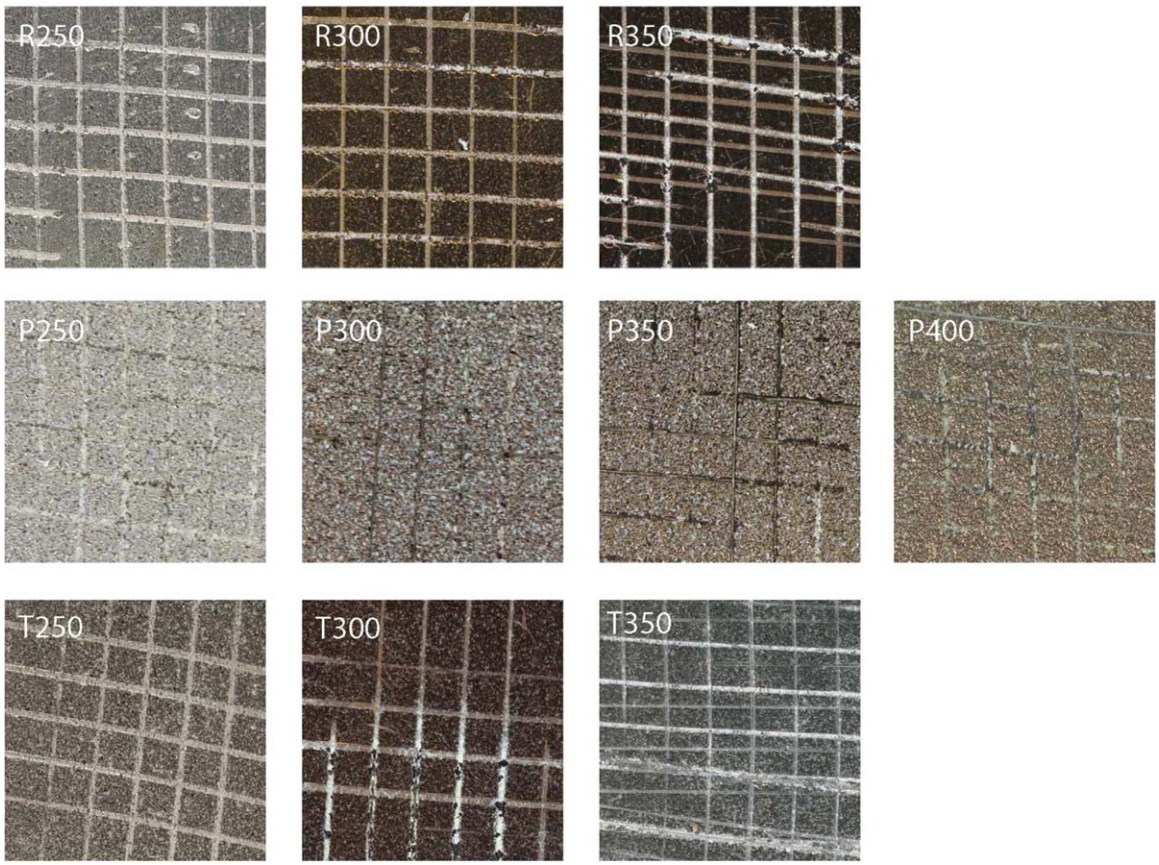

Figure 14. Results of the cross-cut tests performed on the different coatings under investigation. [Color figure can be viewed in the online issue, which is available at wileyonlinelibrary.com.]

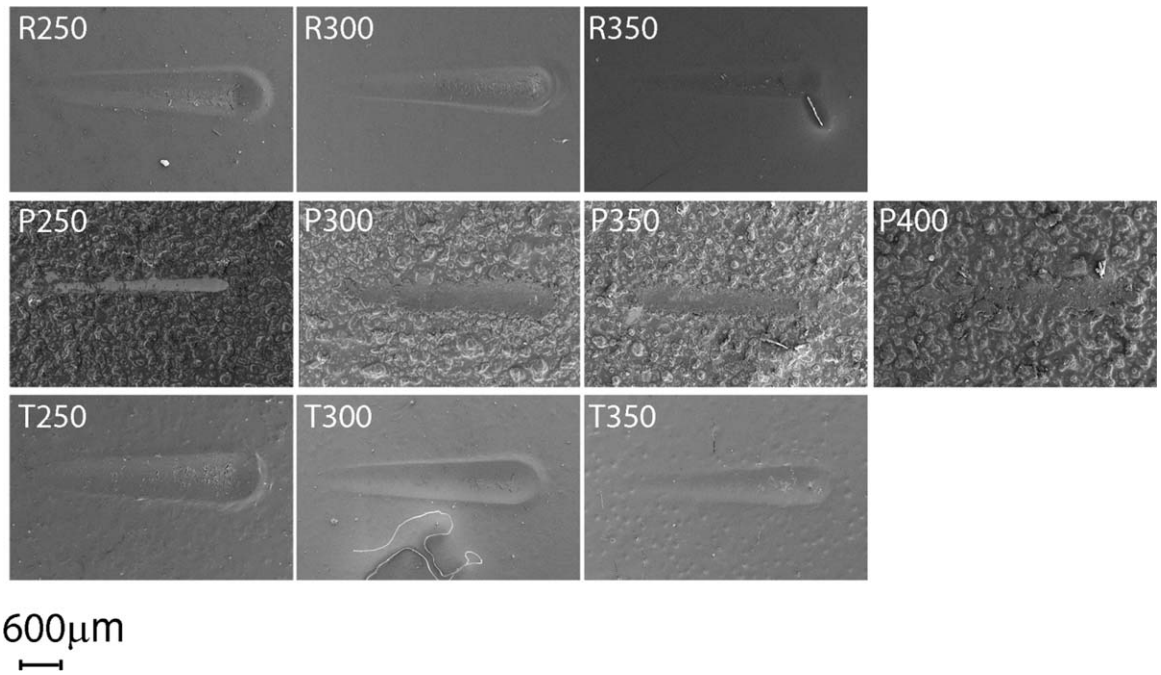

Figure 15. SEM images of the residual scratch patterns after progressive load scratch tests with an increasing load from 0 to 30 N and with an indenter with an 800 µm tip radius.

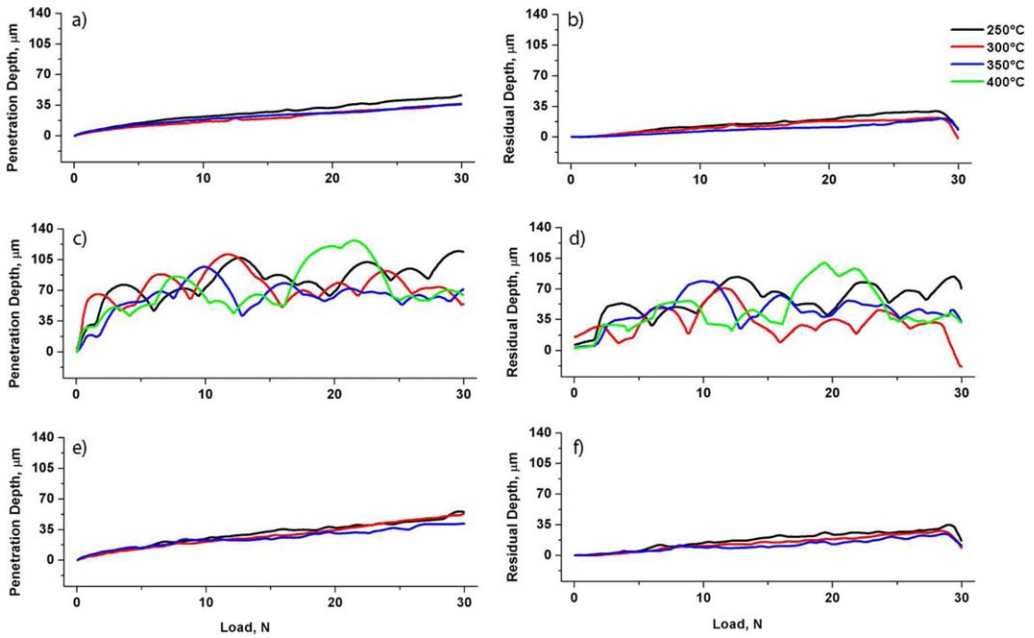

Figure 16. Trends of penetration depths of the coatings after progressive load scratch tests with an increasing load from 0 to 30 N and with an indenter with a 800 μm tip radius: (a, b) Type R250, R300, R350; (c, d) Type P250, P300, P350, P400; (e, f) Type T250, T300, T350. [Color figure can be viewed in the online issue, which is available at wileyonlinelibrary.com.]

plastically displaced materials along the edges of the pattern (i.e., pile-up). Curing temperature plays an analogous influence on the scratch resistance on samples T. Curing at 250 °C leads to coating with the poorest scratch response. The sample T250 features microfractures already at intermediate loads (∼17 N). In this case, the damage is constituted by several microcracks in the bottom of the scratch pattern. A tensile cracking mechanism occurs. The coating material is compressed by the advancing indenter ahead the tip and stretched behind it. When the stresses inside the material overcome the ultimate strength of the coating, the material can fracture as it happens in sample T250 in agreement with the experimental findings in Ref. 43 on a similar MPP resin. An increase in curing temperature to 300 and 350 °C leads to an improvement of MPP performance. The resin features an increment in the cross-linking degree, thus offering an improved cohesive strength. The sample T300 shows onset of failure for applied loads of 20 N. The sample T 350 withstands even higher applied loads (∼23 N). Figure 16(e,f) summarizes the trends of the penetration depths for the double-layered coatings. The tip reaches a maximum penetration depth of 50 μm on the samples T250 and T300, a maximum penetration depth of only 35 μm is observed for the sample T 350, thus confirming the improved scratch response of the coatings cured at the highest temperature.

CONCLUSIONS

This work concerns the manufacturing and characterization of composite PEEK–MPP coatings. Accordingly, the following pointwise conclusions can be drawn:

- Curing temperature of MPP influences cross-linking and mineralization degree of the resin; at the lowest curing temperature, the resin features limited cohesive strength and high ductility; at progressively higher curing temperature, the resin features an increased cohesive strength, with a stiffer and glassy-like response.
- PEEK powders modify the morphology of the coatings, giving rise to corrugated coatings; indeed, PEEK improves the thermal resistance of the coatings by the possible formation of interphases with the MPP resin, which generate a material with good strength at the highest curing temperature.
- Double-layered coatings feature an improved visual appearance because of the MPP topcoat; this topcoat keeps on failing at 400 °C curing temperature because of the brittleness of the polysiloxane resin due to the high degree of cross-linking and mineralization.
- Scratch performance of the samples P400 and T350 are very high, with P400 being extremely resistant and T350 featuring a better visual appearance and good surface smoothness.

In conclusion, liquid-driven spraying deposition of PEEK composite coatings can lead to the built-up and growth of high-performance composite coatings on metal substrate, thus offering a valid alternative to conventional deposition techniques, strongly limited by the scarce interfacial adhesion and compatibility between PEEK and metal as well as by costly and tricky operational procedures.

REFERENCES

1. Simonin, L.; Liao, H. *Macromol. Mater. Eng.* **2000**, *283*, 153.
2. Liao, H.; Beche, E.; Coddet, C. In Coddet, C. Ed., Proceeding of ITSC 1998, ASM International, Materials Park: OH, **1998** *25*
3. Li, J.; Liao, H.; Coddet, C. *Wear* **2002**, *252*, 824.

4. Soveja, A.; Sallamand, P.; Liao, H.; Costil, S. *J. Mater. Process. Technol.* **2011**, *211*, 12.
5. Fauchais, P.; Montavon, G.; Vardelle, M.; Cedelle, J. *Surf. Coat. Technol.* **2006**, *201*, 1908.
6. Zhang, G.; Liao, H.; Li, H.; Mateus, C.; Bordes, J. M.; Coddet, C. *Wear* **2006**, *260*, 594.
7. Boccaccini, R.; Peter, C.; Roether, J. A.; Eifler, D.; Misra, S. K.; Minay, E. J. *J. Mater. Sci.* **2006**, *41*, 8152.
8. Wang, C.; Ma, J.; Cheng, W. *Surf. Coat. Technol.* **2003**, *173*, 271.
9. Patel, K.; Doyle, C. S.; James, B. J.; Hyland, M. M. *Polym. Degrad. Stab.* **2010**, *95*, 792.
10. Hedayati, M.; Salehi, M.; Bagheri, R.; Panjepour, M.; Naeimi, F. *Progr. Org. Coat.* **2012**, *74*, 50.
11. Zhang, G.; Liao, H.; Yu, H.; Ji, V.; Huang, W.; Mhaisalkar, S. G.; Coddet, C. *Surf. Coat. Technol.* **2006**, *200*, 6690.
12. Corni, I.; Neumann, N.; Eifler, D.; Boccaccini, A. R. *Adv. Eng. Mater.* **2008**, *10*, 559.
13. Corni, I.; Neuman, N.; Novak, S.; König, K.; Veronesi, P.; Chen, Q.; Rayan, M. P.; Boccaccini, A. R. *Surf. Coat. Technol.* **2009**, *203*, 1349.
14. Patel, K.; Doyle, C.; Yonekura, D.; James, B. J. *Surf. Coat. Technol.* **2010**, *204*, 3567.
15. Frigione, M. E.; Mascia, l.; Acierno, D. *Eur. Polym. J.* **1995**, *31*, 1021.
16. Pham, S.; Burchill, P. J. *Polymer* **1995**, *36*, 3279.
17. Ollier, R.; Stocchi, A.; Rodriguez, E.; Alvarez, V. *Mater. Sci. Appl.* **2012**, *3*, 442.
18. Jiang, B.; Huang, Y. D.; Wang, Q. *Mater. Res. Exp.* **2014**, *1*, 25.
19. Lee, J. K.; Char, K.; Rhoc, H. W. *Polymer* **2001**, *42*, 9085.
20. Barletta, M.; Gisario, A.; Puopolo, M.; Vesco, S. *Mater. Des.* **2015**, *69*, 130.
21. Mowrer, N. R. Performance Coatings and Finishes, Polysiloxanes; Ameron International: Rancho Cucamonga, California, **2003**.
22. Keijman, J. M. High Solids Coatings: Experience in Europe and USA, In *Proceedings Protective Coatings Europe Conference, Paper 40*, The Hague, The Netherlands, March, **1997**.
23. Cheng, S. Z.; Cao, M. Y.; Wunderlich, B. *Macromolecules* **1986**, *19*, 1868.
24. Ramos, J. A.; Blanco, M.; Zalakain, I.; Mondragon, I. *J. Colloid Interface Sci.* **2009**, *336*, 431.
25. Heilen, W. Silicone Resins and Their Combinations; Vincentz Network GmbH & Co KG: Hannover, Germany, **2005**.
26. Sun, J. T.; Huang, Y. D.; Cao, H. L.; Gong, G. F. *Polym. Degrad. Stab.* **2004**, *85*, 725.
27. Liu, W.; Hu, S.; Liu, G.; Pan, F.; Wu, H.; Jiang, Z.; Wang, B.; Li, Z.; Cao, X. *J. Mater. Chem. A* **2014**, 1.
28. Grill, A. *Mater. Ann. Rev. Mater. Res.* **2009**, *39*, 49.
29. Zhou, W.; Yang, H.; Guo, X.; Lu, J. *Polym. Degrad. Stab.* **2006**, *91*, 1471.
30. Han, Y.; Zhang, J.; Shi, L.; Qi, S.; Cheng, J.; Jin, R. *Polym. Degrad. Stab.* **2008**, *93*, 242.
31. Zheng, Y.; Tan, Y.; Dai, L.; Lv, Z.; Zhang, X.; Xie, Z.; Zhang, Z. *Polym. Degrad. Stab.* **2012**, *97*, 2449.
32. Uricanu, V.; Donescu, D.; Banu, A. G.; Serban, S.; Olteanu, M.; Dudauc, M. *Mater. Chem. Phys.* **2004**, *85*, 120.
33. Voice, A. M.; Bower, D. I.; Ward, I. M. *Polymer* **1993**, *34*, 1164.
34. Huy Nguyen, X.; Hatsuo, I. *Polymer* **1986**, *27*, 1400.
35. Rzatki, F. D.; Barboza, D. V. D.; Schroeder, R. M.; de, G. M.; Barra, O.; Binder, C.; Klein, A. N.; de Mello, J. D. B. *Wear* **2015**, *332–333*, 844.
36. Franquet, A.; De Laet, J.; Schram, T.; Terryn, H.; Subramanian, V.; van Ooij, W. J. *Thin Solid Films* **2001**, *384*, 37.
37. Franquet, A.; Terryn, H.; Vereecken, J. *Thin Solid Films* **2003**, *441*, 76.
38. Keijman, J. M. Properties and Use of Inorganic Polysiloxane Hybrid Coatings for the Protective Coatings Industry, In *2as Jornadas da Revista Corrosao e Proteccao de Materiais*, Lisbon, November, **2000**.
39. Wanga, Y.; James, E.; Ghita, O. R. *Mater. Des.* **2015**, *83*, 545.
40. Bull, S. J. *Surf. Coat. Technol.* **1991**, *50*, 25.
41. Jovanović, Z.; Bajat, J. B.; Jančić-Heinemann, R. M.; Dimitrijević, M.; Mišković-Stanković, V. B. *Progr. Org. Coat.* **2009**, *66*, 393.
42. Zhang, G.; Lia, W. Y.; Cherigui, M.; Zhang, C.; Liao, H.; Bordes, J. M.; Coddet, C. *Progr. Org. Coat.* **2007**, *60*, 39.
43. Barletta, M.; Rubino, G.; Tagliaferri, V.; Vesco, S. *Colloids Surf. A Physicochem. Eng. Asp.* **2014**, *455*, 147.